Novel Computational Probes of Diffusive Motion†

M. Scott Shell,*,‡ Pablo G. Debenedetti,‡ and Frank H. Stillinger§

Department of Chemical Engineering and Department of Chemistry, Princeton University, Princeton, New Jersey 08544

Received: April 4, 2005; In Final Form: June 9, 2005

Self-diffusion constants, *D*, and the atomic-level processes that produce them have been investigated numerically for the binary-mixture Lennard−Jones (BMLJ) model and for liquid silica as described by the Van Beest−Kramer−Van Santen interaction model. The primary conceptual tool for this study is the joint probability distribution for single particles as a function of initial velocity and positional displacement at a given later instant. Self-diffusion constants can be expressed exactly in terms of this probability function. The numerical simulations for the BMLJ case reveal an unusual temperature effect; in contrast to the high-temperature behavior, particles with high initial velocities experience disproportionate retardation in forward displacement. In the silica modeling simulations, diffusive processes have been compared at constant-temperature "isodiffusive" pairs of states, demonstrating a significant role played by the amount of local tetrahedral order that is present in the medium.

I. Introduction

The diffusion of particles within many-body systems, whether gas, liquid, or solid, constitutes one of the most basic kinetic properties of extended matter. This process reveals the capacity of those systems to explore energetically available particle configurations at the prevailing temperature and pressure, and its rate is a sensitive indicator of atomic and/or molecular interactions that are present. Experimental determinations of diffusion constants, and various attempts to supply those measurements with insightful theoretical explanations, have a long and venerable history.[1] But the richness and diversity of the experimental observations, including their considerable variation from one substance to another, have continued to prove to be conceptually challenging to the interested scientific community. In particular, the behavior of diffusion in supercooled liquids, and its connection to shear viscosity through the well-known Stokes−Einstein relation, have provided the focus of numerous publications appearing since the early 1990s.[2]

The primary purpose of this presentation arises from the desirability, if not the necessity, to employ alternative ways of analyzing diffusive particle motions. A previous publication has indicated some tactics of this sort,[3] elements of which are revisited for completeness in the following Section, II. Because the intent is to use these alternatives to analyze results from molecular dynamics computer simulations, Section III outlines two specific models that we have used to study diffusive processes in the liquid state. Results for those models and their interpretation have been collected in Section IV. Several conclusions and suggestions for subsequent study appear in the final Section, V.

II. Formal Relations

The self-diffusion constant, *D*, measures the rate at which particles wander from an initial position as time advances. Let $\mathbf{r}_i(t)$ denote the position of particle *i* at time *t* in an equilibrated many-particle system. Then *D* is determined as follows[4]

$$D = \lim_{t\to\infty} \langle [\Delta \mathbf{r}_i(t)]^2 \rangle / 6t \qquad \text{(II.1)}$$

$$\Delta \mathbf{r}_i(t) = \mathbf{r}_i(t) - \mathbf{r}_i(0)$$

Here the angular brackets denote an ensemble average. Expression II.1 can be converted readily to a velocity autocorrelation function format[4]

$$D = (1/3)\int_0^\infty \langle \mathbf{v}_i(0)\cdot\mathbf{v}_i(t)\rangle \, dt \qquad \text{(II.2)}$$

These two expressions for *D* are standard statistical mechanical representations for this quantity.

An alternative approach considers the mean displacement that a particle, *i*, exhibits at time $t > 0$, having initially possessed velocity, $\mathbf{v}_i(0)$, at $t = 0$. This vector conditional probability will be denoted by the symbol $\langle \Delta\mathbf{r}_i(t)|\mathbf{v}_i(0)\rangle$. It reflects the dynamic interaction of the given particle with its surrounding medium, including dissipation of the initial kinetic energy, and it is an odd function of $\mathbf{v}_i(0)$. The self-diffusion constant can then be obtained as the following integral[3]

$$D = (1/3)\lim_{t\to\infty} \int P_{eq}(\mathbf{v})[\mathbf{v}\cdot\langle \Delta\mathbf{r}(t)|\mathbf{v}\rangle] \, d\mathbf{v} \qquad \text{(II.3)}$$

where particle label *i* has been suppressed for typographical simplicity, and $\mathbf{v}$ stands for $t = 0$ velocity. The Maxwell−Boltzmann velocity distribution at thermal equilibrium has been denoted by

$$P_{eq}(\mathbf{v}) = (m/2\pi k_B T)^{3/2} \exp(-mv^2/2k_B T) \qquad \text{(II.4)}$$

III. Simulation Procedures

For one portion of our molecular dynamics simulations, we analyzed the binary mixture of Lennard−Jones (BMLJ) particles developed by Kob and Andersen,[5] which extended a previous model of an $Ni_{80}P_{20}$ alloy introduced by Weber and Stillinger.[6]

† Part of the special issue "Irwin Oppenheim Festschrift".

* Corresponding author. E-mail: shell@princeton.edu.
‡ Department of Chemical Engineering.
§ Department of Chemistry.

10.1021/jp0517145 CCC: $30.25
Published on Web 07/14/2005

On account of the asymmetry in size and interaction energy between its two components, this system is relatively easy to supercool in simulation and has been studied extensively as a model glass-former.[7−9] In particular, the BMLJ has been found to exhibit pronounced caging and spatially heterogeneous dynamics near its mode-coupling temperature, $T_{MCT} \approx 0.435$.[7,9] This temperature corresponds to that obtained from a power-law fit of measured diffusion constants, although recent analytical calculations suggest an alternative mode-coupling temperature around $T = 0.9$.[10] The mixture consists of two types of particles, A and B, in mole fractions of $x_A = 0.8$ and $x_B = 0.2$. The generic form of the pairwise interaction potential is

$$v_{\alpha\beta}(r) = 4\epsilon_{\alpha\beta}[(\sigma_{\alpha\beta}/r)^{12} - (\sigma_{\alpha\beta}/r)^{6}] \qquad \text{(III.1)}$$

where the subscripts α and β indicate the species identity of the particles, and the associated parameters are $\epsilon_{AA} = 1.0$, $\epsilon_{AB} = 1.5$, $\epsilon_{BB} = 0.5$, $\sigma_{AA} = 1.0$, $\sigma_{AB} = 0.8$, and $\sigma_{BB} = 0.88$. The particle masses are unity for both species. In the present work, all quantities are reported as dimensionless in terms of the AA interactions.

Our molecular dynamics simulations were performed for a total of $N = 250$ particles subjected to cubic periodic boundary conditions. Calculations of dynamic quantities were performed in the microcanonical ensemble; however, equilibration at each temperature was attained by first using a Nose−Hoover thermostat[11−13] over the course of a long trajectory, with a brief subsequent microcanonical equilibration. The equations of motion were integrated using the velocity Verlet algorithm with a time step of 0.003 units. We truncated and shifted each pair potential at $2.5\sigma_{AA}$.

Of central interest in this study has been the time dependence of the particle-averaged function defined by

$$\langle \mathbf{v}_0 \cdot \Delta\mathbf{r} \rangle(t) = \frac{1}{N}\sum_{i=1}^{N} \mathbf{v}_i(0) \cdot \Delta\mathbf{r}_i(t) \qquad \text{(III.2)}$$

which is related directly to the convergence of the integral in eq II.3 as the limit of infinite time taken. Equivalently, this expression converges to the self-diffusion constant according to

$$D = \lim_{t\to\infty} \frac{1}{3}\langle \mathbf{v}_0 \cdot \Delta\mathbf{r} \rangle(t) \qquad \text{(III.3)}$$

In our simulations, we computed the right-hand side of eq III.2 separately for each of the A and B particles. In the results discussed below, we report calculations only for the more populous A species. In addition to this quantity, we also measured the joint distribution of $\Delta\mathbf{r}$ and $\mathbf{v}_0$ for a given fixed offset in time. That is, we measured the continuous probability distribution $P[\Delta x(t), v_x(0)]$ where Δx is the displacement in one of the components of $\Delta\mathbf{r}$ after a time, t, and v_x is the initial velocity of the particle at $t = 0$ along the same axis. Because the liquid is isotropic, results for each of the three components are combined to provide estimates for P. For notational convenience, we will write this distribution in shorthand as $P[\Delta x, v_0]$ with the implicit assumption that Δx and v_0 correspond to the same components of the final displacement and initial velocity vectors. The diffusion constant is related to the long-time behavior of the following moment of this distribution

$$D = \lim_{t\to\infty} \int \mathrm{d}v_0 \int \mathrm{d}\Delta x \{P[\Delta x, v_0]\, \Delta x\, v_0\} \qquad \text{(III.4)}$$

As explained above, we measured the distribution separately for the two species and report the results for the A particles. Algorithmically, both $\langle \mathbf{v}_0 \cdot \Delta\mathbf{r} \rangle$ and $P[\Delta x, v_0]$ were determined by periodically measuring the positions relative to multiple time origins in the molecular dynamics trajectory. These quantities were typically averaged using approximately 1000−10 000 time origins, each separated by 0.1−0.01 time units. This somewhat large number of initial positions was necessary to reduce the large amount of statistical uncertainty in eq III.2 at long times due to the decorrelation of $\mathbf{v}_0$ with growing $\Delta\mathbf{r}$.

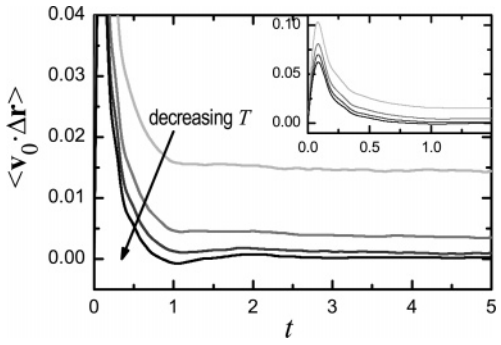

Figure 1. Time evolution of the state average $\langle \mathbf{v}_0 \cdot \Delta\mathbf{r} \rangle$ for A particles in the Lennard−Jones binary mixture, reported for the temperatures $T = 0.44$, 0.50, 0.60, and 0.80. The quantity $\mathbf{v}_0$ is the initial velocity vector of a particle at time $t = 0$ and $\Delta\mathbf{r}$ is the displacement of the same particle after a time $t = \Delta t$ has elapsed. Many time origins, each separated by 0.1 time units, are used over the course of the molecular dynamics trajectories to reduce statistical noise in these calculations.

We also used this type of analysis to investigate self-diffusion in molten silica, SiO_2. Liquid silica possesses an isothermal diffusivity maximum, which renders possible the study of paired isodiffusive points, that is, a pair of densities at the same temperature for which the diffusion constant is the same. A previous study involving two of us has investigated the SiO_2 diffusivity maximum in detail.[14] On the basis of that work, we chose two isodiffusive pairs for the current investigation: at $T = 4000$ K, $\rho_1 = 3800$ kg/m^3, and $\rho_2 = 3000$ kg/m^3; and at $T = 2500$ K, $\rho_1 = 3880$ kg/m^3, and $\rho_2 = 3000$ kg/m^3. We performed molecular dynamics simulations using the pairwise additive potential developed by Van Beest, Kramer, and Van Santen (BKS).[15] This potential treats silica as a mixture of silicon and oxygen ions and includes Coulombic interactions plus an exponential-6 repulsive-dispersive term. Details of the treatment of the potential and simulation methods appear in ref 13. Analogous to the BMLJ calculations, we determined $\langle \mathbf{v}_0 \cdot \Delta\mathbf{r} \rangle$ and $P[\Delta x, v_0]$ for the oxygen ions in liquid silica using multiple time origins every 10 fs.

IV. Numerical Results

The formalism outlined in Section II provides a recipe for determination of the self-diffusion coefficient in simulations, in terms of velocity-displacement correlations in the liquid. Naturally, the first aspect of this new approach we sought to characterize was its convergence properties, namely, the time dependence of the quantity $\langle \mathbf{v}_0 \cdot \Delta\mathbf{r} \rangle$. Figure 1 shows the results for this quantity measured at temperatures ranging from moderately hot ($T = 0.8$) to deeply supercooled ($T = 0.44$) in the BMLJ system. The general form of the $\langle \mathbf{v}_0 \cdot \Delta\mathbf{r} \rangle$ versus t curve in each case is the following. Starting at a value of zero at $t = 0$, there exists a rapid, initially linear increase in this quantity triggered by the short-time ballistic motion of particles. The initial slope of this region is related to the temperature because

$$\langle \mathbf{v}_0 \cdot \Delta\mathbf{r} \rangle \approx \langle \mathbf{v}_0 \cdot \mathbf{v}_0 \delta t \rangle = (k_B T/m)\delta t \qquad \text{(IV.1)}$$

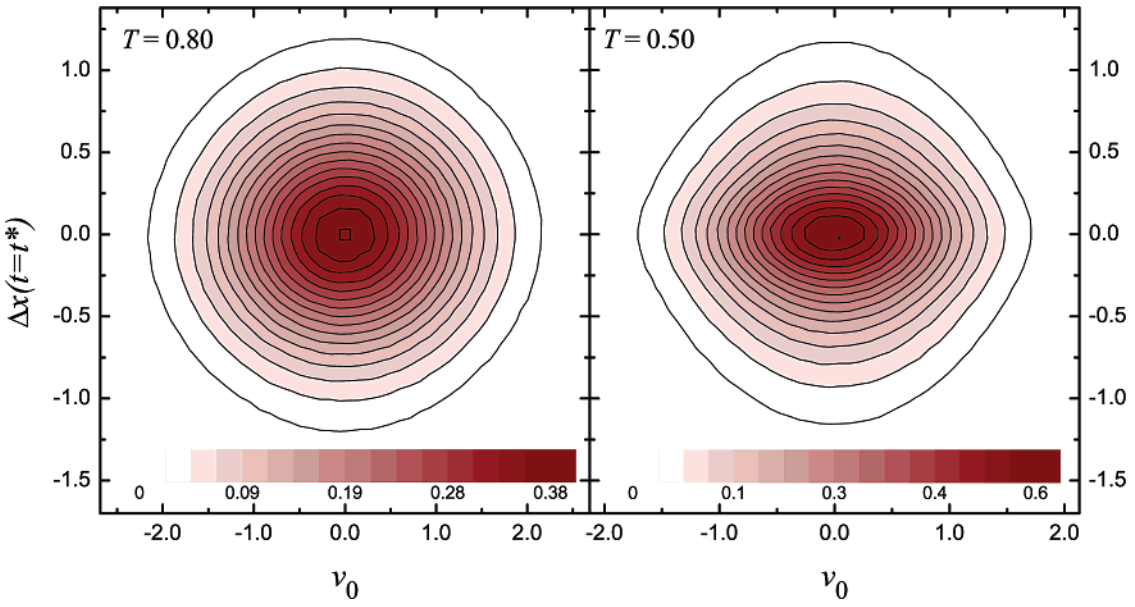

Figure 2. Contour plot representation of the joint distribution $P[\Delta x, \upsilon_0]$ for A particles in the binary system at two different temperatures. This continuous probability function gives the fraction of particles $P\ \mathrm{d}v_0\ \mathrm{d}\Delta x$ with initial momentum $\upsilon_0 \pm \mathrm{d}\upsilon_0$ in the direction of x and with an eventual displacement $\Delta x \pm \mathrm{d}\Delta x$ along the same axis. The shadings yield different values of the height of P. The time at which the particle displacements are analyzed, t^*, corresponds to that at which the average distance traveled by all particles is equal to the mean particle diameter: $t^* = 24$ for $T = 0.8$ and $t^* = 627$ for $T = 0.5$. At lower temperatures, the contours develop a pronounced distortion that shifts their shape from circular to diamond.

However, eventually this ballistic motion ceases, owing to the inevitable collisions a particle will experience when it travels a sufficient distance to probe the repulsive core of its neighbors. Thus at longer times, $<\mathbf{v}_0\cdot\Delta\mathbf{r}>$ reaches a pronounced maximum with a subsequent decay to a constant asymptotic value, the final value being related to the diffusion coefficient (see eq III.3). Figure 1 shows that the location of this maximum in time is relatively insensitive to the temperature; this is a particularly interesting feature given that the diffusion constant spans over 2 orders of magnitude for the temperatures reported. One might hypothesize that the maximum is related to the time it takes a single particle to encounter substantial resistance along its travel direction from its neighbors, and thus is somewhat analogous to the mean-free path picture in gases. An alternative analogy might invoke the Einstein model of solids in which short-time particle displacements are described as harmonic oscillations about local potential energy wells. Notably, the frequency of such harmonic oscillators is insensitive to temperature, instead depending only on the particle masses and the curvature around the potential energy minima.

At the lowest temperature studied, $T = 0.44$, which is only slightly above the mode-coupling temperature, $\langle\mathbf{v}_0\cdot\Delta\mathbf{r}\rangle$ in Figure 1 briefly becomes negative before finally reaching its long-time positive value. This intermediate excursion into negative values of $\langle\mathbf{v}_0\cdot\Delta\mathbf{r}\rangle$, corresponding to an anticorrelation between displacement and initial velocity, appears to be a signature of caging phenomena in the liquid. Physically, these negative values indicate a "rebound" effect of a particle encountering an effective wall or cage formed by its environment. The possibility exists that this effect persists in several additional "rebounding" motions which yield a subtle, damped oscillatory behavior in the $\langle\mathbf{v}_0\cdot\Delta\mathbf{r}\rangle$ calculations, which are almost evident in our measurements but are obscured by statistical noise.

The logistical aspects of the calculations presented in Figure 1 require some commentary. This set of data required very large numbers of time origins in order to reduce statistical errors due to the effects of fluctuations. That occurs because as the elapsed time increases, the displacement of a particle from its initial position in any given realization continues to grow, despite the fact that $\langle\mathbf{v}_0\cdot\Delta\mathbf{r}\rangle$ reaches an asymptotic value. To illustrate the difficulty, we consider the following simplified scenario in which the displacement can be strictly broken into correlated and uncorrelated portions. After a very long time, many multiples of the relaxation time of the system, we might write this quantity as

$$\langle\mathbf{v}_0\cdot\Delta\mathbf{r}\rangle \approx \langle\mathbf{v}(0)\rangle\cdot\langle\Delta\mathbf{r}_1(\tau)\rangle + \langle\mathbf{v}(0)\rangle\cdot\langle\Delta\mathbf{r}_2(t-\tau)\rangle \quad \text{(IV.2)}$$

where τ is the correlation time, $\Delta\mathbf{r}_1$ is the portion of the overall $\Delta\mathbf{r}$ which is correlated with $\mathbf{v}(0)$, and $\Delta\mathbf{r}_2$ is the strictly uncorrelated portion. Thus, in principle, the last term on the right-hand side of this expression should vanish because of the average over $\Delta\mathbf{r}_2$ in the isotropic liquid. In numerical simulations, however, this term represents an average over quantities that are growing with time, and at very long times, the fluctuations in the displacement vectors tend to introduce substantial noise in the calculation. In the present study, this required on the order of 10^4 time origins to gain reasonably converged data.

The fluctuations themselves, however, are also of great interest to this work. If one considers a particular offset in time, the relevant measure of these fluctuations is the distribution of particles as a function both of their initial velocity at $t = 0$ and their final displacement at $t = \Delta t$. This is a quantity we have also measured for the BMLJ system, and representative calculations at two temperatures are shown in Figure 2. As one would expect, each distribution is peaked around the origin because, in the isotropic liquid, no particular initial velocity or final displacement is favored. There is, however, an extremely subtle skew to the data, which reflects the correlation of $\Delta\mathbf{r}$ with $\mathbf{v}_0$ as given by the expression in eq III.4. The faintness of this skew underscores the need for extremely high-resolution measurements with multiple time origins for determining the quantities in Figure 1. Beyond the value of the self-diffusion constant, these joint distributions contain important information about mechanisms of molecular motions in the liquid. For example,

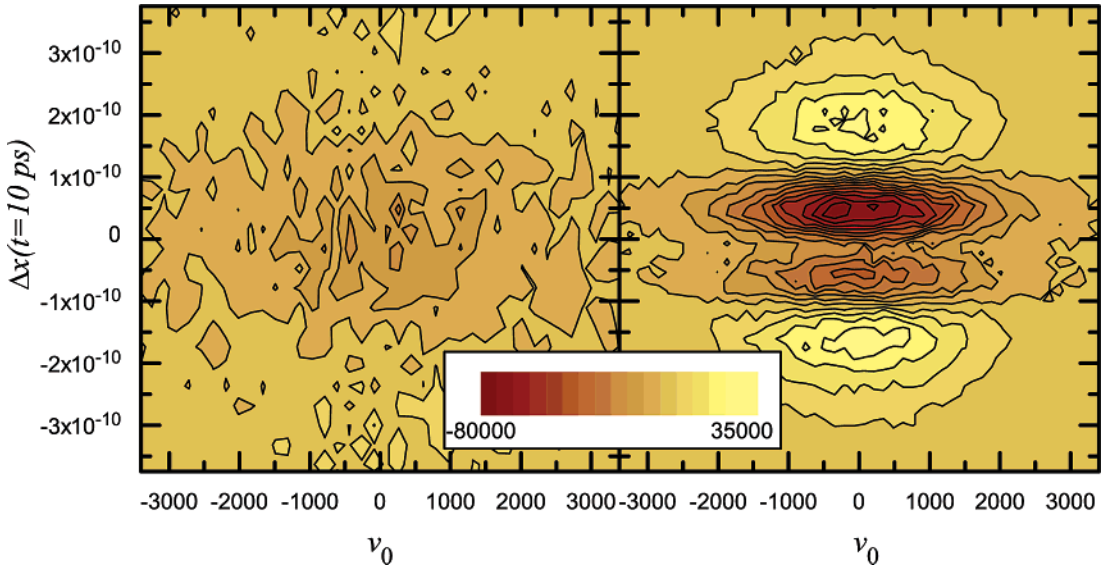

Figure 3. Contour plot of the difference $P_1[\Delta x, v_0] - P_2[\Delta x, v_0]$ for oxygen motions in liquid silica at two densities that possess the same diffusion constant (i.e., two isodiffusive points). The plot to the left corresponds to $T = 4000$ K, for which $\rho_1 = 3800$ kg/m^3 and $\rho_2 = 3000$ kg/m^3, and the one to the right is for $T = 2500$ K, with $\rho_1 = 3880$ kg/m^3 and $\rho_2 = 3000$ kg/m^3.

one can calculate the non-Gaussian parameter[16] for the distribution of particle displacements by integrating over the velocity component. This parameter has been identified as a signature of supercooled dynamics and has been studied previously for the BMLJ model in ref 9. Although we will leave this kind of analysis for future work, the present formalism allows one to understand the combined role of particle velocity and displacement in the emergence of non-Gaussian behavior.

The results in Figure 2 stem from two of the temperatures studied, $T = 0.8$ and $T = 0.5$ in the left and right panels, respectively. Each of these sets of data corresponds to the joint distribution of displacement and initial velocity after a fixed time offset, t^*, which depends on the temperature. We have selected t^* to be the time displacement at which the average distance traveled by a particle is equivalent to an average particle diameter (calculated using the conformal relation $\bar{\sigma}^3 = x_A^2\sigma_{AA}^3 + x_Ax_B\sigma_{AB}^3 + x_B^2\sigma_{BB}^3$). Figure 2 shows that, as the temperature is decreased toward the mode-coupling temperature, the qualitative shape of the velocity-displacement distribution changes from nearly symmetric with circular contours to an unusual diamond-like shape. The persistence of this behavior even with nontrivial particle motion (each particle traveling one diameter on average) makes it an effective signature of qualitatively distinct dynamical processes occurring in the supercooled liquid. The diamond shape implies that at low temperatures, particles with extreme initial velocities are not able to travel as far as their counterparts in the hot liquid. That is, the effects of these rare velocities are more readily dampened by interactions with their surrounding neighbors. We are currently investigating the diffusive mechanisms that give rise to the diamond shape.

To make a more drastic illustration of the mechanistic insight that the current formalism provides, we have performed similar calculations on a model of liquid silica. Specifically, we have determined the joint velocity-displacement distributions at state points in the liquid that have the same temperature and diffusion constant but differ in densities by roughly 25%; these are the isodiffusive state pairs discussed in the preceding Section, III. One expects the mechanism of diffusion to be distinct for the two densities; at the lower one, silica readily forms local tetrahedrally arranged structures using Si−O−Si links, whereas repulsive interactions disrupt this tetrahedrality at higher densities.[14] This distinction in structural ordering is generally more pronounced at lower temperatures, where the propensity for adopting local tetrahedral arrangements at low bulk densities becomes stronger. In the present work, we fix the temperature and examine the difference in the velocity-displacement distribution between the two densities. Figure 3 shows the results of this exercise at high ($T = 4000$ K, left panel) and at low ($T = 2500$ K, right panel) temperatures. The results indicate the emergence of significant differences in diffusive motion as the temperature is lowered, marked by the development of peaks and valleys in this graph. It appears that the high-density mechanism leads to an increased number of particles with near-zero initial velocity that are able to travel farther. At the lower density, the tendency of these particles to travel shorter distances may be some indication of the constraining effects of the tetrahedral network.

V. Conclusions and Discussion

The macroscopic manifestation of diffusion that is described by Fick's law at large time and length scales is deceptively simple. But hidden within that law's phenomenological self-diffusion constant, D, are extraordinarily complex many-body dynamical processes. Details of this complexity control the dependence of D on the substance involved and on the thermodynamic state of that substance through the local interparticle interactions that are present, and through the local order of those particles as they respond to their interactions. The result of this interplay is that D can vary over many orders of magnitude even for a single substance, an observation that is especially noticeable for liquids that can be supercooled toward a glass transition.

Both laboratory experiments and computer simulations have historically offered a variety of probes for the microscopic details of diffusive motions in fluids, but in some respects the conceptual picture remains incomplete. The project reported in this paper has been directed toward filling the knowledge gap at least to a modest extent. Attention here has focused on the probability distribution for the displacement of a particle during a time interval, t, provided that its velocity vector at the beginning of the interval was given. Equation II.3 above indicates how this conditional probability yields D, an expression

trivially related to the usual statistical mechanical expressions for that quantity.[4] The advantage of the present formulation is that it can appeal to the intuitive notion of local mean viscous dissipation of initial particle velocity, a connection originally embodied in the approximate but appealing Stokes−Einstein relation.

By numerically examining the form of the joint probability distribution for initial particle velocity and the position displacement at a later time, we have uncovered nontrivial and perhaps unexpected aspects of the diffusion process complexity for the binary-mixture Lennard−Jones (BMLJ) model, and the Van Beest−Kramer−Van Santen model for molten silica. For the former model, the comparison of results displayed in Figure 2 indicates that lowering the temperature has the effect of substantially changing the local viscoelastic response of the surrounding liquid medium to the disturbing initial motion of a test particle. In particular, at low temperature, rapid initial velocity is "counterproductive" because the surroundings statistically cannot move quickly enough to get out of the way to permit substantial forward displacement to occur. The silica model permits numerical comparisons for isodiffusive pairs of states, for which the oxygen D is the same at distinctly different densities (but the same temperature). The probability difference plots presented in Figure 3 illustrate the role of local tetrahedral order in the diffusive process and how isodiffusive compression alters that role. These examples appear to support the notion that the approach advocated in this paper, centered on the joint distribution of initial particle velocity and time-lagged mean particle displacement, is a useful computational strategy.

The results reported in this paper appear to be sufficiently encouraging to justify application to other types of models, and perhaps even to diffusion in other phases (crystals, surface films, etc.). In addition, some other details of the approach would probably be useful to examine. One is to explore the joint velocity-displacement probability in the large initial velocity limit. Of course the Maxwell−Boltzmann velocity distribution, eq II.4, assigns very low probability to such circumstances at thermal equilibrium. However, experimental techniques conceivably could be designed to produce anomalously high particle velocity in an otherwise normal equilibrated liquid. It would be a significant contribution to the theory to understand how the surrounding medium reacts to the large perturbation produced by an extreme single-particle velocity, a circumstance easy to arrange in a numerical simulation. Another direction for extension would be the "isotope effect": how does the joint velocity-displacement distribution depend on the mass of the particle involved?[17] Once again, it is straightforward to investigate this effect in numerical simulation, and even to vary the "tagged" particle mass over a much wider range than real isotopes would permit in experiments.

Acknowledgment. P.G.D. gratefully acknowledges financial support by the U.S. Department of Energy, Division of Chemical Sciences, Geosciences, and Biosciences, Office of Basic Energy Sciences, grant no. DE-FG02-87ER13714. M.S.S. gratefully acknowledges the support of the Fannie and John Hertz Foundation.

References and Notes

(1) Einstein, A. *Ann. Phys. (Weinheim, Ger.)* **1905**, *17*, 549; Einstein, A. *Ann. Phys. (Weinheim, Ger.)* **1906**, *19*, 289; Einstein, A. *Ann. Phys. (Weinheim, Ger.)* **1906**, *19*, 371; Einstein, A. *Ann. Phys. (Weinheim, Ger.)* **1911**, *34*, 591.

(2) (a) Fujara, F.; Geil, B.; Sillescu, H.; Fleischer, G. Z. *Z. Phys. B: Condens. Matter* **1992**, *88*, 195. (b) Chang, I.; Fujara, F.; Geil, B.; Hueberger, G.; Mangel, T.; Sillescu, H. *J. Non-Cryst. Solids* **1994**, *172/174*, 248. (c) Stillinger, F. H.; Hodgdon, J. A. *Phys. Rev. E* **1994**, *50*, 2064. (d) Cicerone, M.; Ediger, M. D. *J. Chem. Phys.* **1996**, *104*, 7210. (e) Jung, Y.; Garrahan, J. P.; Chandler, D. *Phys. Rev. E* **2004**, *69*, 061205.

(3) Stillinger, F. H.; Debenedetti, P. G. *J. Phys. Chem. B* **2005**, *109*, 6604.

(4) Hansen, J. P.; McDonald, I. R. *Theory of Simple Liquids*, 2nd ed; Academic Press: New York, 1986; Chapter 7.

(5) Kob, W.; Andersen, H. C. *Phys. Rev. Lett.* **1994**, *73*, 1376.

(6) Weber, T. A.; Stillinger F. H. *Phys. Rev. B* **1985**, *31*, 1954.

(7) Kob, W.; Andersen, H. C. *Phys. Rev. E* **1995**, *51*, 4626.

(8) Sampoli, M.; Benassi, P.; Eramo, R.; Angelani, L.; Ruocco, G. *J. Phys.: Condens. Matter* **2003**, *15*, S1227.

(9) Kob, W.; Donati, C.; Plimpton, S. J.; Poole, P. H.; Glotzer, S. C. *Phys. Rev. Lett.* **1997**, *79*, 2827.

(10) Brumer, Y.; Reichman, D. R. *Phys. Rev. E*, **2004**, *69*, 041202.

(11) Nose, S. *J. Chem. Phys.* **1984**, *81*, 511.

(12) Nose, S. *Mol. Phys.* **1984**, *52*, 255.

(13) Hoover, W. G. *Phys. Rev. A* **1985**, *31*, 1695.

(14) Shell, M. S.; Debenedetti, P. G.; Panagiotopoulos, A. Z. *Phys. Rev. E* **2002**, *66*, 011202.

(15) Van Beest, B. W. H.; Kramer, G. J.; Van Santen, R. A. *Phys. Rev. Lett.* **1990**, *64*, 1955.

(16) Rahman, A. *Phys. Rev. Lett*. **1964**, *136*, A405.

(17) Habdas, P.; Schaar, D.; Levitt, A. C.; Weeks, A. R. *Europhys. Lett.* **2004**, *67*, 477.